EUROPEAN JOURNAL OF PURE AND APPLIED MATHEMATICS
2025, Vol. 18, Issue 3, Article Number 6481
ISSN 1307-5543 – ejpam.com
Published by New York Business Global

Fractional Discrete Modeling and Numerical Analysis of Hepatitis B and C Dynamics with Neural Network Approximation

Sajid Ali Shah[1], Nasir Rehman[2], Sadique Ahmad[3,*],Mohammed A.Elaffendi[3], Abdelhamied Ashraf Ateya[3]

[1] *Department of Zoology Government Degree College Thana Malakand, Khyber Pakhtunkhwa, Pakistan*
[2] *Department of Mathematics, Allama Iqbal Open University Islamabad, Pakistan*
[3] *EIAS Data Science and BlockChain Laboratory, College of Computer and Information Sciences, Prince Sultan University, Riyadh 11586, Saudi Arabia*

Abstract. This paper is devoted to establish a details analysis for the dynamics of hepatitis B and C through some mathematical difference equations. Serious viral illnesses that mainly affect the liver, hepatitis B and C can cause inflammation and even damage to the liver. Hepatitis B can spread by bodily fluids such as semen or vaginal fluid, even though both are blood-borne. While hepatitis C can be cured with medication, hepatitis B can be prevented with vaccine. We formulate a mathematical model of the mentioned disease through fractional difference equations using the Caputo fractional difference operator (CFDO). Existence theory, Ulam-Hyers (UH) stability and numerical investigation are deduced. Further, analysis based on artificial intelligence (AI) is considered. We have used neural networks (NNs) based investigations to conduct our study. Various graphical illustrations are given to demonstrate our results. For our analysis we use Matlab software with 2023 version.

2020 Mathematics Subject Classifications: 26A33, 34A08, 68T07, 92B20

Key Words and Phrases: Viral infections, Difference equations, Numerical investigation, Neural networks.

1. Introduction

A well-known area of study in the biological sciences, epidemiology looks at health, disease, and associated variables at the population level. The science of epidemiology is primarily concerned with human populations, as evidenced by the fact that the term

*Corresponding author.
DOI: https://doi.org/10.29020/nybg.ejpam.v18i3.6481

Email addresses: shahsajidali442@gmail.com (S. A. Shah), nasir.rehman@aiou.edu.pk (N. Rehman),saahmad@psu.edu.sa (S. Ahmad), Affendi@psu.edu.sa (M. A. Affendi), aateya@psu.edu.sa (A. A.ateya)

"epidemiology" is formed from three Greek words: epi (upon), demos (public), and logos (research) [1]. Nowadays, there is a wealth of opportunities to use mathematical research in the biological sciences to the study of infectious diseases. Both human and non-human populations' rates of illness and mortality are greatly influenced by infectious diseases. As a result, both mathematicians and biologists are interested in the potential of formal models to alleviate these pressures [2]. In the field of mathematical biology, numerous scholars have devoted their time to investigating the transmission of infectious illnesses using a variety of well-established mathematical models [3]. Throughout history, infectious diseases have had a significant impact on people's lives. In many parts of the world, infectious diseases that manifest as outbreaks cause pandemic that claim millions of lives. For example, the 1918 influenza virus [4], commonly referred to as "the Spanish Flu," produced the greatest pandemic in recorded history before COVID-19 [5]. Over 50 million people died globally during the aforementioned outbreak. Since the spread of susceptible and ill individuals might infect more people and potentially result in their death, infectious diseases have long posed a threat to human safety [6].

Globally, between 64 and 103 million people have a chronic infection. Unsterile medical procedures, iatrogenic infections, and inappropriate injectable drug use are key risk factors for HCV infection in countries where it is extremely prevalent. In regions with high HCV incidence, unsterile medical procedures (iatrogenic infections) and improper injectable drug use are major risk factors for these blood-borne viral infections [7]. Hepatitis B is a viral disease that can cause liver failure, cirrhosis, and liver cancer. More than 250 million persons worldwide are estimated to have a chronic Hepatitis B infection by the World Health Organization (WHO) [8]. Hepatitis C is a virus that can cause liver cancer, cirrhosis, and liver failure. Over 70 million people worldwide suffer from a chronic Hepatitis C infection, according to the WHO [9]. Hepatitis B and C are major public health concerns in Pakistan. According to a nationwide survey conducted by the Pakistan Medical Research Council (PMRC) in 2017-18, the prevalence of Hepatitis B and C in the general population aged 15 and older was estimated to be 2.5% and 4.8%, respectively [10].

It is crucial to remember that when real-world issues are represented in terms of mathematical equations, they become more effective instruments for comprehending phenomena. The study of mathematical epidemiology has drawn much more attention in the last 200 years [11]. Numerous infectious diseases have been studied using the concept of mathematical biology. Much research effort has been focused on the aforementioned field. Kermack-McKendrick created a simple mathematical model called susceptible, infected, and recovered (SIR). Only infection and removal events are included in this model, which is adequate to explain a basic epidemic, including the threshold condition required for an epidemic to start (see [12]). Mathematical modeling is a very clever tool that scientists and engineers use to solve real-world problems [13]. Recently, fractional calculus has been used in modeling real world problems interms of fractional difference equations (FDEs). The literature has put forth a number of definitions of fractional-order operators, each with unique advantages and disadvantages. As a logical progression of the integer-order difference equation, one such operator is called a fractional-order discrete difference opera-

tor. Since real-world data is usually in discrete form, these operators work incredibly well for researching real-world phenomena since they produce output in the discrete form. Image processing[14] , game theory[15], ecology[16], neural networks[17], epidemiology[18], economics[19], and electrical engineering[20] are just a few of its many uses. Recently, researchers have explored the area further and produced significant results, we refer to [21, 22].

Because it makes it easier to evaluate experimental results and comprehend the biological mechanisms driving epidemic spread, mathematical modeling is a valuable tool for studying virus dynamics. Theoretical biologists can better understand the processes that contribute to the disease by using mathematical models to study the dynamics of the Hepatitis B virus. Numerous models have been proposed to comprehend the dynamics of Hepatitis B and C. Authors have studied the model [23] for Hepatitis B and C given by

$$\begin{cases} \dot{H}(t) = \Lambda - \delta H - \eta HV, \\ \dot{I}(t) = \eta HV - \gamma I, \\ \dot{V}(t) = \lambda I - \mu V, \\ H(0) = H_0,\ I(0) = I_0,\ V(0) = V_0, \end{cases} \tag{1}$$

where H stands for healthy cells, I for infected and V for virus free cells density respectively. Λ is the birth rate, η is efficacy rate of the process to infection, δ, μ and γ stand for death rates respectively of healthy, infected and virus free cells respectively. In addition, λ is the free virus cell production rate. We extend the model (1) under the Caputo fractional difference operator as described by

$$\begin{cases} {}^{C}\Delta^{\xi} H(t) = \Lambda - \delta H(t+\xi-1) - \eta H(t+\xi-1)V(t+\xi-1), \\ {}^{C}\Delta^{\xi} \mathrm{I}(t) = \eta H(t+\xi-1)V(t+\xi-1) - \gamma I(t+\xi-1), \\ {}^{C}\Delta^{\xi} \mathrm{R}(t) = \lambda I(t+\xi-1) - \mu V(t+\xi-1), \end{cases} \tag{2}$$

where $t \in [0, b]_{\mathbb{N}_0}$. We describe the formulation (2) in schematic diagram as given in figure 1.

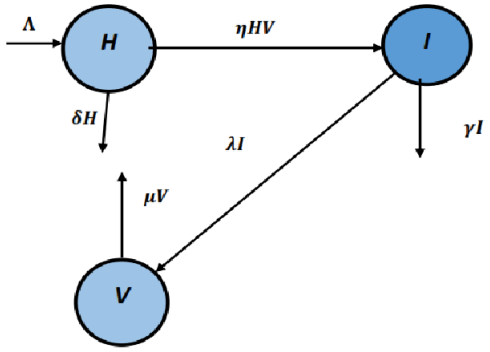

Figure 1: Schematic diagram of model (2).

We use fixed point theorem to deduce the existence theory for model (2). Also, numerical analysis against various fractional orders has been given. UH stability is also deduced for the considered model. In addition, in recent time AI tools based NNs have attracted attention to use in investigation of different epidemic models. Large amounts of data are utilized to train data-driven neural networks, which can be used to build mathematical models and solve inverse problems [24]. Data-driven neural networks can assist in improving the current models and equations and obtaining an equation that describes the process being studied. Deep learning techniques can be used to do this. For instance, authors [25] was suggested to use deep learning to forecast how many people in various parts of the US would contract COVID-19 and pass away over the course of one to four weeks. AI models based on deep neural networks and epidemic compartmental models based on differential equations are effective tools for assessing and preventing the spread of viral infectious disease like HBV and HCV. However, the difficulties in estimating parameters restrict the potential of compartmental models, and AI models are unable to identify the evolutionary pattern of said disease and are not explainable [26, 27]. The concerned NNs are consisted on multi layers including input output layers. The structure of such NNs, we can describe as in figure 3.

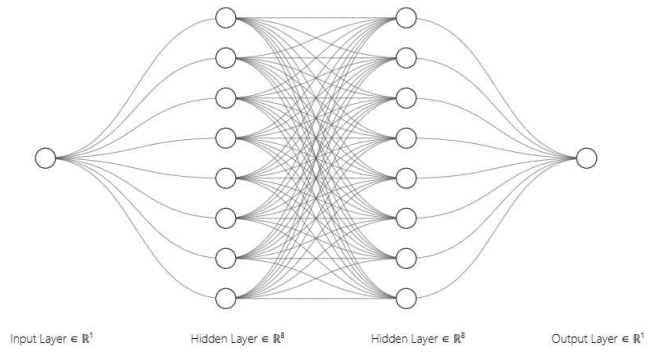

Figure 2: Structure of NNs.

With the help of mentioned NNs, we deduce some analysis for the concerned model by computing the root mean square (RMS) and mean square error (MSE) as well as regression coefficient R. Neural networks learn, optimize, and forecast using a variety of algorithms. Back propagation, gradient descent, and its variations, such as Adam and Stochastic Gradient Descent (SGD), are important algorithms. Convolutional neural networks (CNNs), recurrent neural networks (RNNs), and long short-term memory (LSTM) networks are further significant methods. Neural models are trained using the Liveners-Marquardt backward propagation algorithm (LMBA). Recently, researchers have used NNs and fractional calculus to investigate various problems, we refer to [28–30].

2. Basic Results

Some basic results are demonstrated below.

Definition 1. *[18] For function $\chi(t)$, the ξ-CFDO is defined by*

$$ {}^{C}\Delta_a^{\xi}\chi(t) = \Delta_a^{-(\mathrm{n}-\xi)}\Delta^{\mathrm{n}}\chi(t) = \frac{1}{\Gamma(\mathrm{n}-\xi)}\sum_{\mathrm{s}=a}^{t-(\mathrm{n}-\xi)}(t-\mathrm{s}-1)^{\mathrm{n}-\xi-1}\Delta^{\mathrm{n}}\chi(\mathrm{s}), \tag{3} $$

where $t \in \mathbb{N}_{a+\mathrm{n}-\xi}, \mathrm{n} = \lceil \xi \rceil + 1$ and $\xi > 0$ with $\xi \notin \mathbb{N}$ and $(t-1-\mathrm{s})^{(\mathrm{n}-\xi-1)}$, while the n-the integer difference operator denoted by $\Delta^{\mathrm{n}}\chi(\mathrm{s})$ which can be expressed as follows:

$$ (t-\mathrm{s}-1)^{(\mathrm{n}-\xi-1)} = \frac{\Gamma(t-\mathrm{s})}{\Gamma(t-\mathrm{s}-\mathrm{n}+\xi+1)}, \tag{4} $$

and

$$ \Delta^{\mathrm{n}}\chi(t) = \Delta(\Delta^{\mathrm{n}-1}\chi(t)) = \sum_{\mathrm{k}=0}^{\mathrm{n}}\binom{\mathrm{n}}{\mathrm{k}}(-1)^{\mathrm{n}-\mathrm{k}}\chi(t+\mathrm{k}), \quad t \in \mathbb{N}_a. \tag{5} $$

Remark 1. *For* $\mathrm{n}=1$*, the* ξ*-CFDO is defined as:*

$$ {}^{C}\Delta_a^{\xi} f(t) = \Delta_a^{-(1-\xi)} \Delta\chi(t) = \frac{1}{\Gamma(1-\xi)} \sum_{\mathrm{s}=a}^{t-(1-\xi)} (t-\mathrm{s}-1)^{-\xi} \Delta\chi(\mathrm{s}), \tag{6} $$

where $t \in \mathbb{N}_{a+1-\xi}$.

Definition 2. *[18] With the mapping* $\chi : \mathbb{N}_a \to \mathbb{R}$*, let* $\chi(t)$ *be a function defined on* $\mathbb{N}_a$*. The following is the definition of the* ξ*-the fractional sum of* f *in this context:*

$$ \Delta^{-\xi}\chi(t) = \frac{1}{\Gamma(\xi)} \sum_{\mathrm{s}=a}^{t-\xi} (t-\mathrm{s}-1)^{\xi-1} \chi(\mathrm{s}), \tag{7} $$

where $\xi > 0, t \in \mathbb{N}_{b+\xi} = \{b+\xi, b+\xi+1, \dots\}$ *is a time scale and* $b \in \mathbb{R}$.

Lemma 1. *[19] Let* $\xi > 0$ *and* χ *be defined on* $\mathbb{N}_a$*, then:*

$$ \begin{aligned} \Delta^{-\xi C}\Delta^{\xi}\chi(t) &= \chi(t) - \textstyle\sum_{\mathrm{k}=0}^{\mathrm{n}-1} \frac{(t-b)^{(\mathrm{k})}}{\mathrm{k}!} \Delta^{\mathrm{k}} h(b) \\ &= f(t) + c_0 + c_1 t + \cdots + c_{\mathrm{n}} t^{\mathrm{n}-1}, \end{aligned} $$

such that n *satisfies* $\mathrm{n} \geq \xi$ *and* $c_i \in \mathbb{R},\ i = 1, 2, \dots, \mathrm{n}-1$.

Lemma 2. *[19] The following equality holds:*

$$ \sum_{\mathrm{s}=0}^{t-\xi} (t-\mathrm{s}-1)^{(\xi-1)} = \frac{\Gamma(t+1)}{\xi\Gamma(t-\xi+1)}. \tag{8} $$

The proposed model (2) can be written as follows:

$$ \begin{cases} H(t) = H(0) + \dfrac{1}{\Gamma(\xi)} \displaystyle\sum_{s=1-\xi}^{t-\xi} (t-s-1)^{\xi-1} (\Lambda - \eta H(t+\xi-1)V(t+\xi-1) - \delta H(t+\xi-1)) \\ I(t) = I(0) + \dfrac{1}{\Gamma(\xi)} \displaystyle\sum_{s=1-\xi}^{t-\xi} (t-s-1)^{\xi-1} (\eta H(t+\xi-1)V(t+\xi-1) - \gamma I(t+\xi-1)), \\ V(t) = V(0) + \dfrac{1}{\Gamma(\xi)} \displaystyle\sum_{s=1-\xi}^{t-\xi} (t-s-1)^{\xi-1} (\lambda I(t+\xi-1) - \mu V(t+\xi-1). \end{cases} \tag{9} $$

3. Existence and Uniqueness

Take model (9) in the following form

$$ \begin{cases} \chi_1(t+\xi-1, H, I, V) = \Lambda - \eta H(t+\xi-1)V(t+\xi-1) - \delta H(t+\xi-1), \\ \chi_2(t+\xi-1, H, I, V) = \eta H(t+\xi-1)V(t+\xi-1) - \gamma I(t+\xi-1), \\ \chi_3(t+\xi-1, H, I, V) = \lambda I(t+\xi-1) - \mu V(t+\xi-1), \end{cases} \tag{10} $$

then equation (9) may be described as

$$g(t) = g(0) + \frac{1}{\Gamma(\xi)} \sum_{\mathrm{s}=0}^{t-\xi} (t - \mathrm{s} - 1)^{\xi-1} F(\mathrm{s} + \xi - 1, g(\mathrm{s} + \xi - 1)), \tag{11}$$

while

$$g(t) = \begin{cases} H(t) \\ I(t) \\ V(t) \end{cases}, \quad g(0) = \begin{cases} H_0 \\ I_0 \\ V_0 \end{cases}, \quad F(t+\xi-1, g(t+\xi-1)) = \begin{cases} \chi_1(t+\xi-1, H, I, V) \\ \chi_2(t+\xi-1, H, I, V) \\ \chi_3(t+\xi-1, H, I, V) \end{cases} \tag{12}$$

The following fixed-point theorems must be applied in order to prove the existence and uniqueness of solutions for the system (9).

Theorem 1. *[27] A contraction mapping established on a complete metric space has exactly one fixed point, according to the unique fixed point feature.*

Theorem 2. *[27] . This means that ψ has at least one fixed point in D if $\psi : D \subseteq \mathbb{R}^n \to D \subseteq \mathbb{R}^n$ is a continuous mapping defined on a nonempty, bounded, closed, and convex set D.*

We define the Banach space by $X = \mathbb{X}_1 \times \mathbb{X}_2 \times \mathbb{X}_3$ such that $\mathbb{X}_i$, $(i = 1, 2, 3)$ are sequences of real numbers $(H, I, V) = \{H(t), I(t), V(t)\}_{t=\xi-1}^{b+\xi}$ under the norm $\|g\| = \|(H, I, V)\| = \sup_{t\in[\xi-1,b+\xi]_{\mathbb{N}_{\xi-1}}} [|H(t)| + |I(t)| + |V(t)|]$. Then $\psi X \to X$ such that

$$(\psi g)(t) = g(0) + \frac{1}{\Gamma(\xi)} \sum_{\mathrm{s}=0}^{t-\xi} (t - \mathrm{s} - 1)^{\xi-1} F(\mathrm{s} + \xi - 1, g(\mathrm{s} + \xi - 1)). \tag{13}$$

Define $D_\psi = \max\left\{\frac{\Gamma(t+1)}{\Gamma(\xi+1)\Gamma(t-\xi+1)}\right\} = \frac{\Gamma(b+\xi+1)}{\Gamma(\xi+1)\Gamma(b+1)}$.

Theorem 3. *Let*

$(\mathbf{C}_1)$ *: We have bounded function $\mathcal{F} : [\xi - 1, b + \xi]_{\mathbb{N}_{\xi-1}} \to \mathbb{R}$ with $\big|F(t, g)\big| \leq \mathcal{F}(t)\big|g\big|$ at every $g \in X$.*

The system (2) *has at least one solution at X, if $\mathcal{F}^* < D_\psi$, with $\mathcal{F}^* = \max\{\mathcal{F}(t) : t \in [\xi - 1, b + \xi]_{\mathbb{N}_{\xi-1}}\}$.*

Proof. Take $\mathcal{P} > 0$ such that $U = \big\{g\big|[\xi - 1, b + \xi]_{\mathbb{N}_{\xi-1}} \to \mathbb{R}, \|g\| \leq \mathcal{M}\big\}$, we need to show that ψ maps U into U. For any $g \in U$, we have

$$\begin{aligned} \big|(\psi g)(t)\big| &\leq \frac{\mathcal{F}(t)}{\Gamma(\xi)} \sum_{\mathrm{s}=0}^{t-\xi} (t - \mathrm{s} - 1)^{\xi-1} \big|g(\mathrm{s} + \xi - 1)\big|, \\ &\leq \frac{\mathcal{F}(t)\|g\|}{\Gamma(\xi)} \sum_{\mathrm{s}=0}^{t-\xi} (t - \mathrm{s} - 1)^{\xi-1}, \end{aligned}$$

$$\leq D_{\psi}\mathcal{F}^{*}\mathcal{P}.$$

Thus $|(\psi g)(t)| < \mathcal{P}$, then $\|(\psi g)\| \leq \mathcal{P}$ implies that ψ maps U to itself. On using Theorem (2), ψ has at least one solution. Hence system (2) has also at least one solution.

Theorem 4. *Let*

($\mathbf{C}_2$) *: If there exists constant* $\mathcal{K} > 0$ *such that* $\big|F(t,g) - F(t,\bar{g})\big| \leq \mathcal{K}\big|g - \bar{g}\big|$ *at all* $t \in [\xi - 1, b + \xi]_{\mathbb{N}_{\xi-1}}$ *and* $g, \bar{g} \in X$.

The system (2) *has a unique solution on* X *if* $\mathcal{K} < D_{\psi}$.

Proof. If $g, \bar{g} \in X$, then for every $t \in [\xi - 1, b + \xi]_{\mathbb{N}_{\xi-1}}$ such that

$$\begin{aligned}
\big|(\psi g)(t) - (\psi\bar{g})(t)\big| &\leq \frac{1}{\Gamma(\xi)}\sum_{\mathrm{s}=0}^{t-\xi}(t - \mathrm{s} - 1)^{\xi-1}\big|F(\mathrm{s} + \xi - 1, g(\mathrm{s} + \xi - 1)) \\
&\quad - G(\mathrm{s} + \xi - 1, g(\mathrm{s} + \xi - 1))\big|, \\
&\leq \frac{\mathcal{F}}{\Gamma(\xi)}\sum_{\mathrm{s}=0}^{t-\xi}(t - \mathrm{s} - 1)^{\xi-1}\big|g(\mathrm{s} + \xi - 1)) - \bar{g}(\mathrm{s} + \xi - 1))\big|, \\
&\leq \frac{\mathcal{F}\|g - \bar{g}\|}{\Gamma(\xi)}\sum_{\mathrm{s}=0}^{t-\xi}(t - \mathrm{s} - 1)^{\xi-1}, \\
&\leq D_{\psi}\mathcal{F}\|g - \bar{g}\|.
\end{aligned}$$

Thus $\|(\psi g) - (\psi\bar{g})\| \leq \|g - \bar{g}\|$, Since ψ is a contraction, there is a unique fixed point of ψ that is also a unique solution of the system (2) according to the Banach fixed-point theorem (1).

Here, we deduce some results for stability analysis.

$$|{}^{C}\Delta^{\xi}g(t) - F(\mathrm{s} + \xi - 1, g(\mathrm{s} + \xi - 1))| \leq \epsilon, \quad t \in [0, b]_{\mathbb{N}_0}. \tag{14}$$

Definition 3. *[28] The problem* (2) *is UH stable for any* $\epsilon > 0$*, if we have a constant* $D_g > 0$ *which obeys the inequality* (14) *such that*

$$|g(t) - \bar{g}(t)| \leq D_g\epsilon, \quad t \in [\xi - 1, b + \xi]_{\mathbb{N}_{\xi-1}}. \tag{15}$$

The generalization of equation (2) If the constant $D_g\epsilon$ in inequality (14) is replaced by the function $\phi(\epsilon)$, UH stability is maintained, where $\phi \in C(\mathbb{R}^{+}, \mathbb{R}^{+})$ and $\phi(0) = 0$.

Remark 2. *If* $g \in X$ *is a solution to inequality* (14) *and there exists* $\Theta : [\xi - 1, b + \xi]_{\mathbb{N}_{\xi-1}} \to \mathbb{R}$, $\ni$

(i) $|\Theta(\mathrm{s} + \xi - 1)| \leq \epsilon, \quad t \in [0, b]_{\mathbb{N}_0}$,

(ii) ${}^{C}\Delta^{\xi}g(t) = F(\mathrm{s} + \xi - 1, g(\mathrm{s} + \xi - 1)) + \Theta(\mathrm{s} + \xi - 1), \quad t \in [0, b]_{\mathbb{N}_0}$.

Theorem 5. *In view of* $(\mathbf{C}_2)$*, the suggested model* (2) *is UH stable if* $\mathcal{K} < D_{\psi}^{-1}$.

Proof. Take $g, \bar{g} \in X$ be the solution of equation (2) using the Remark 2, one has

$$g(t) = g(0) + \frac{1}{\Gamma(\xi)} \sum_{\mathrm{s}=0}^{t-\xi} (t - \mathrm{s} - 1)^{\xi-1} F(\mathrm{s} + \xi - 1, g(\mathrm{s} + \xi - 1)) + \Theta(\mathrm{s} + \xi - 1). \tag{16}$$

In view of Remark 2, for $t \in [\xi - 1, b + \xi]_{\mathbb{N}_{\xi-1}}\}$, we get

$$\left\| g(t) - \left(g(0) + \frac{1}{\Gamma(\xi)} \sum_{\mathrm{s}=0}^{t-\xi} (t - \mathrm{s} - 1)^{\xi-1} F(\mathrm{s} + \xi - 1, g(\mathrm{s} + \xi - 1)) \right) \right\| \leq D_{\psi}\epsilon. \tag{17}$$

For $t \in [\xi - 1, b + \xi]_{\mathbb{N}_{\xi-1}}$, one has

$$\begin{aligned} |g(t) - \bar{g}(t)| &= \left| g(t) - \left(g(0) + \frac{1}{\Gamma(\xi)} \sum_{\mathrm{s}=0}^{t-\xi} (t - \mathrm{s} - 1)^{\xi-1} F(\mathrm{s} + \xi - 1, g(\mathrm{s} + \xi - 1)) \right) \right|, \\ &\leq D_{\psi}\epsilon + \frac{1}{\Gamma(\xi)} \sum_{\mathrm{s}=0}^{t-\xi} (t - \mathrm{s} - 1)^{\xi-1} \\ &\quad \times |F(\mathrm{s} + \xi - 1, g(\mathrm{s} + \xi - 1)) - F(\mathrm{s} + \xi - 1, \bar{g}(\mathrm{s} + \xi - 1))|, \\ &\leq D_{\psi}\epsilon + \frac{1}{\Gamma(\xi)} \sum_{\mathrm{s}=0}^{t-\xi} (t - \mathrm{s} - 1)^{\xi-1} \mathcal{K} \|g - \bar{g}\| \end{aligned} \tag{18}$$

which further means

$$\|g - \bar{g}\| \leq \left[\frac{D_{\psi}}{1 - \mathcal{K} D_{\psi}} \right] \epsilon = D_g \epsilon. \tag{19}$$

Also set $D_g = \frac{D_{\psi}}{1 - \mathcal{K} D_{\psi}} > 0$, we conclude that solution of (2) is UH stable. It is possible to determine that the solution of model (2) satisfies the requirements for generalized UH stability by choosing $\phi(\epsilon) = D_g \epsilon$, where $\phi(0) = 0$.

4. Qualitative Results of Model (2)

Here, we deduce some results related to positivity, equilibrium points and reproductive number. Also, stability result is deduced. We see that from Eq.(9)

$$H(t) = H(0) + \frac{1}{\Gamma(\xi)} \sum_{s=1-\xi}^{t-\xi} (t - s - 1)^{\xi-1} (\Lambda - \eta H(t + \xi - 1) V(t + \xi - 1) - \delta H(t + \xi - 1)) > 0$$

$$I(t) = I(0) + \frac{1}{\Gamma(\xi)} \sum_{s=1-\xi}^{t-\xi} (t - s - 1)^{\xi-1} (\eta H(t + \xi - 1) V(t + \xi - 1) - \gamma I(t + \xi - 1)) > 0,$$

$$V(t) = V(0) + \frac{1}{\Gamma(\xi)} \sum_{s=1-\xi}^{t-\xi} (t - s - 1)^{\xi-1} (\lambda I(t + \xi - 1) - \mu V(t + \xi - 1) > 0,$$

which implies that $H(t),\ I(t),\ V(t)$ are positive for $t > 0$. The disease free E_0 and endemic E^* equilibrium points are computed as follows: $E_0 = (H_0, I_0, V_0) = \left(\frac{\Lambda}{\delta}, 0, 0\right)$, and $E^* = (H^*, I^*, V^*)$, where

$$H^* = \frac{\gamma\mu}{\eta\lambda},\ I^* = \frac{\mu(\lambda\eta\Lambda - \delta\gamma\mu)}{\lambda^3\eta},\ V^* = \frac{\lambda\eta\Lambda - \delta\gamma\mu}{\lambda^2\eta}.$$

Further, the reproductive number is computed as

$$\mathcal{R}_0 = \frac{\eta\Lambda\lambda}{\delta\gamma\mu}.$$

Theorem 6. *The point E_0 is asymptotically stable if $\mathcal{R}_0 < 1$.*

Proof. From the Jacobian matrix J at E_0, we have

$$\det(J - \rho I) = \begin{vmatrix} \rho + \delta & 0 & \frac{\eta\Lambda}{\delta} \\ 0 & \rho + \gamma & -\frac{\eta\Lambda}{\delta} \\ 0 & \lambda & \rho + \mu \end{vmatrix} = 0$$

which yields that $\rho = -\delta < 0$, and $\rho^2 + a_1\rho + a_2 = 0$, where $a_1 = \gamma + \mu,\ a_2 = \frac{\gamma\delta\mu - \Lambda\lambda\eta}{\eta}$, clearly $a_1 > 0$ and $a_2 > 0$ if and only if $\mathcal{R}_0 < 1$.

Theorem 7. *The point E^* is locally asymptotically stable if $\mathcal{R}_0 \geq 1$.*

Proof. The endemic equilibrium point is given by $E^* = (1.0714285714, 0.0849560567, 0.0004757539)$. The characteristic equations becomes $\det(J(E^*) - \rho\mathrm{I}) = 0$. Upon computation, we get eigens values as

$$\rho_1 = -0.0345678 - 0.0543217\iota,\ \rho_2 = -0.0453276 + 0.079805412\iota,\ \rho_3 = -0.005123984 + 0\iota.$$

We see that all eigen's values have negative real parts. Thus the said equilibrium point is locally asymptotically stable.

5. Numerical Analysis

We reset the system (9) at $\mathrm{s} + \xi = k$ to get the following system

$$\begin{cases} H(\mathrm{n}) = H(0) + \dfrac{1}{\Gamma(\xi)} \displaystyle\sum_{k=1}^{\mathrm{n}} \frac{\Gamma(\mathrm{n} - k + \xi)}{\Gamma(\mathrm{n} - k + 1)} (\Lambda - \eta H(k-1)I(k-1) - \delta H(k-1)), \\ I(\mathrm{n}) = I(0) + \dfrac{1}{\Gamma(\xi)} \displaystyle\sum_{k=1}^{\mathrm{n}} \frac{\Gamma(\mathrm{n} - k + \xi)}{\Gamma(\mathrm{n} - k + 1)} (\eta H(k-1)I(k-1) - \gamma I(k-1)), \\ V(\mathrm{n}) = V(0) + \dfrac{1}{\Gamma(\xi)} \displaystyle\sum_{k=1}^{\mathrm{n}} \frac{\Gamma(\mathrm{n} - k + \phi)}{\Gamma(\mathrm{n} - k + 1)} (\lambda I(k-1) - \mu V(k-1)). \end{cases} \tag{20}$$

We take the initial values in millions as $H(0) = 10, I(0) = 2,\ V(0) = 5$, and $\lambda = 0.0003, \Lambda = 0.02,\ \delta = 0.0001, \eta = 0.0025, \gamma = 0.05, \mu = 0.0056$. We present the numerical interpretation for the three classes in figures 3 and figure 4 for different fractional order values.

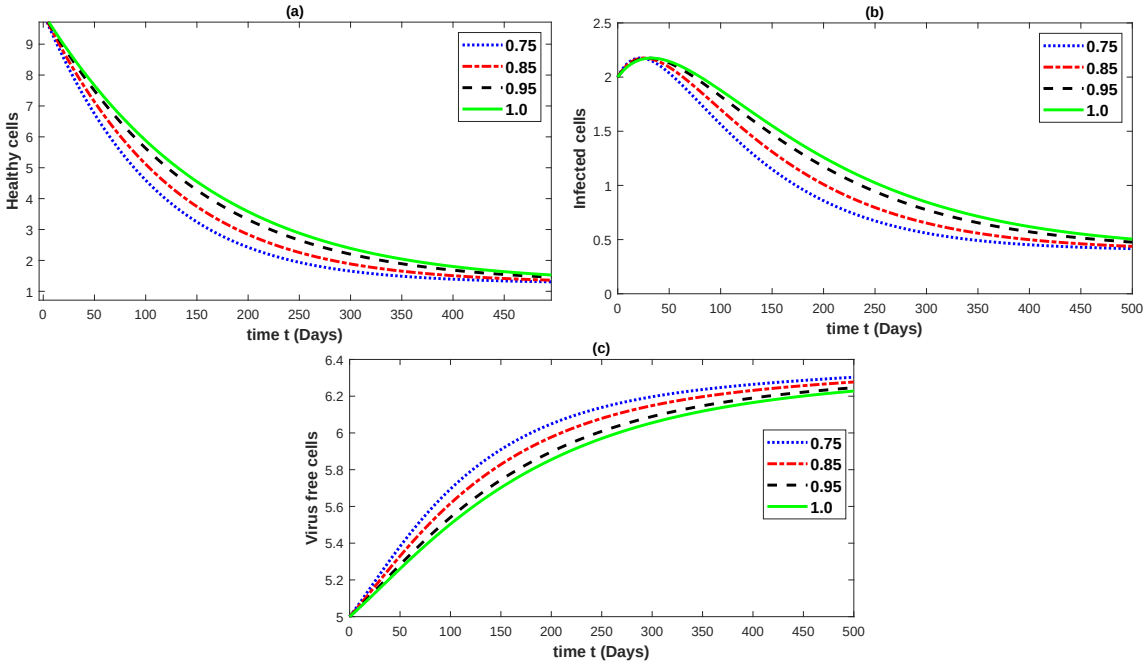

Figure 3: Graphical presentations of approximate solutions using different fractional orders in $[0.75, 1.0]$ for model (2) .

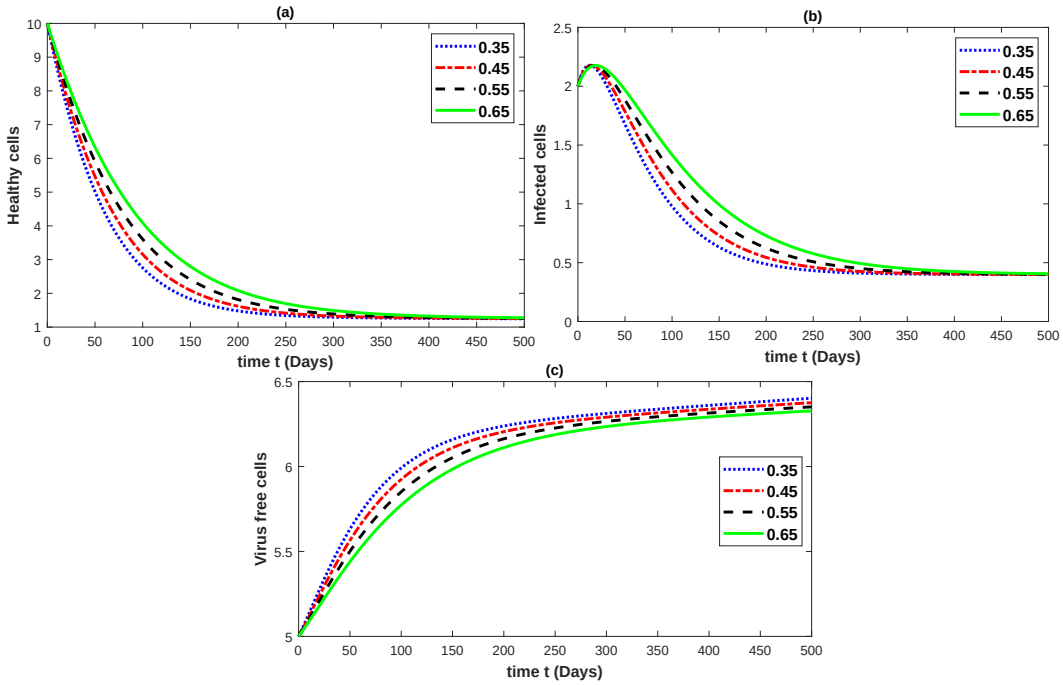

Figure 4: Graphical presentations of approximate solutions using different fractional orders in $[0.35, 0.65]$ for model (2) .

In above both figures 3, 4, we see that density of healthy cells is decreasing with different fractional order until achieve stable position. In the same way, the infected cells density is first rising exponentially and then it goes on decreasing with the passage of time under various fractional order. The density of virus free cells is gradually rising until reaches to a stable position by using different fractional order.

6. NNs Analysis of Model (2)

Here, we demonstrate the analysis based on AI NNs tools. We compute the MSE, RMSE and regression coefficient. The circuit diagram of the concerned NNs is given in figure 5.

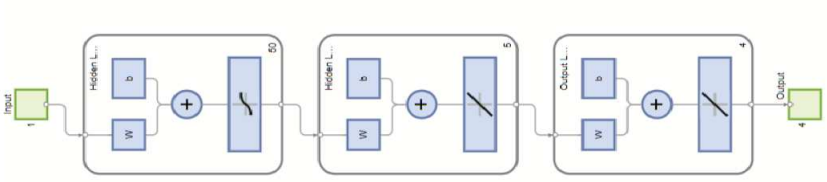

Figure 5: Diagram of neural network that we have used.

Onward, we presents the graphical illustrations of various data including all data, test data, validation and train data. Also the function fit for the given compartments have been presented. In figure 6 sub plots $(a)-(d)$, we have presented all data, test data, validation of data and train data for the density of healthy cells using adopted NNs. Further, in sub plot (e) of figure 6, we have presented the absolute error plots between the numerical and and NNs data analysis, we see that error is very low which shows the best performance of our methodology. Also, the function fits corresponding to various data has given in subplot (f) of figure 6. Further, we have used NNs with two hidden layers of 20 neurons. For other units, we give table 1.

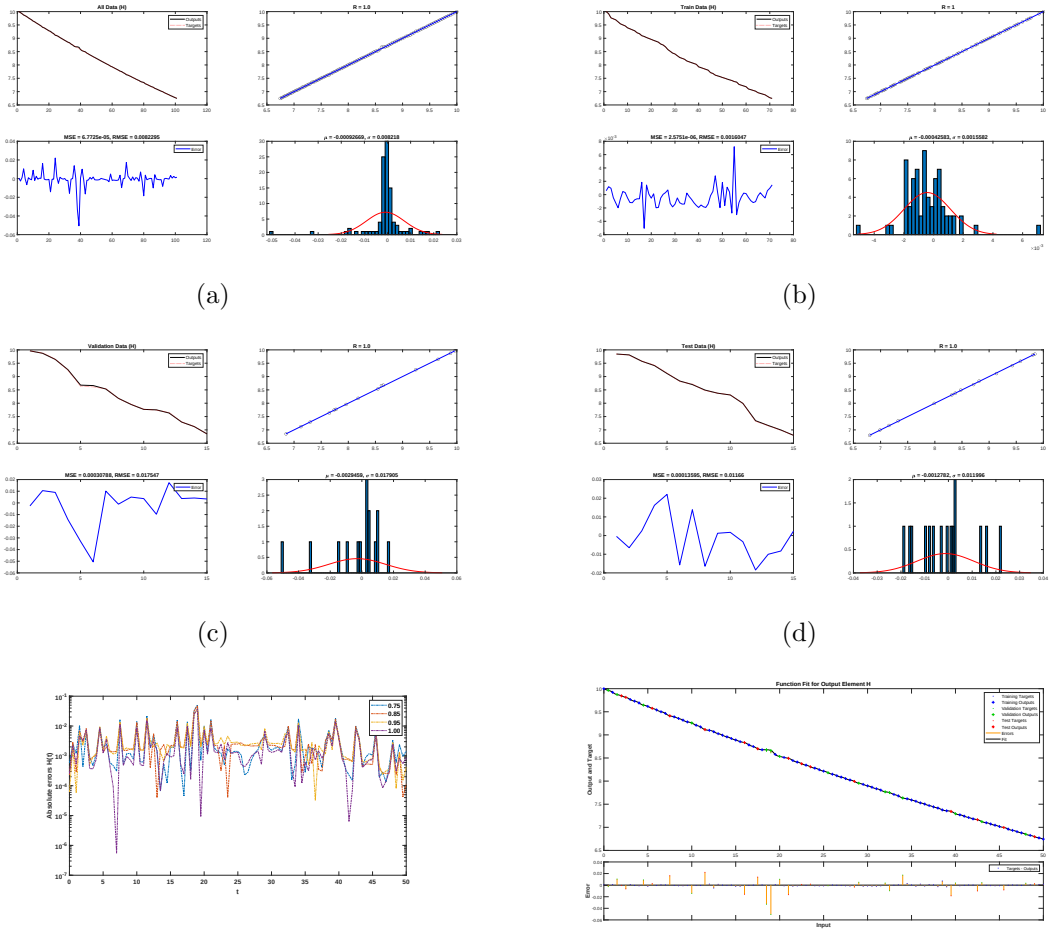

Figure 6: Graphical presentation of various data results for class H using NNs (a) all data, (b) train data, (c) test data (d) validation (e) absolute error using NNs and (f) function fit performance.

Unite	Initial value	stopped value	target value
Epoch	0	11	1000
Elapsed time	-	00:00:00	-
Performance	24.9	$4.06e-11$	0
Gradient	41.7	$6.53e-05$	$1e-07$
standard deviation	0.001	$1e-11$	$1e+11$
Validation checks	0	6	6

Table 1: Training progress presentation for class H.

In figure 7 sub plots $(a)-(d)$, we have presented all data, test data, validation of data and train data for the density of infected cells using adopted NNs. Further, in sub plot (e) of figure 7, we have presented the absolute error plots between the numerical and and NNs data analysis, we see that error is very low which shows the best performance of our methodology. Also, the function fit of class I corresponding to various data has given in subplot (f) of figure 7. The NNs used contain two hidden layers with 20 neurons, while other units are presented in table 2.

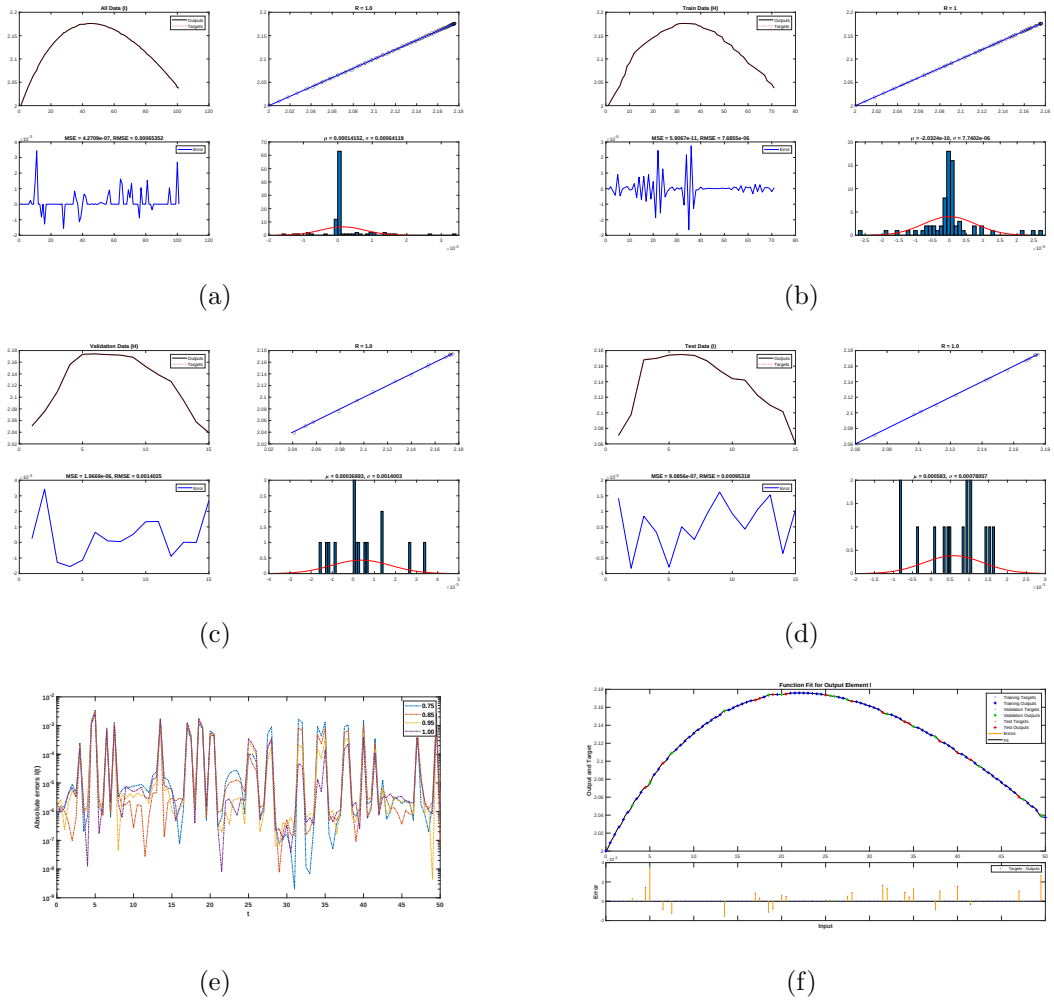

Figure 7: Graphical presentation of various data results for class H using NNs (a) all data, (b) train data, (c) test data (d) validation (e) absolute error using NNs and (f) function fit performance.

Unite	Initial value	stopped value	target value
Epoch	0	17	1000
Elapsed time	-	00:00:00	-
Performance	33.7	$2.96e-09$	0
Gradient	56	$9.73e-08$	$1e-07$
standard deviation	0.001	$1e-09$	$1e+10$
Validation checks	0	0	6

Table 2: Training progress presentation for class I.

In figure 8 sub plots $(a)-(d)$, we have presented all data, test data, validation of data and train data for the density of virus free cells using adopted NNs. Further, in sub plot (e) of figure 8, we have presented the absolute error plots between the numerical and and NNs data analysis, we see that error is very low which shows the best performance of our methodology. Also, the function fit for virus free cells density corresponding to various data has given in subplot (f) of figure 8.

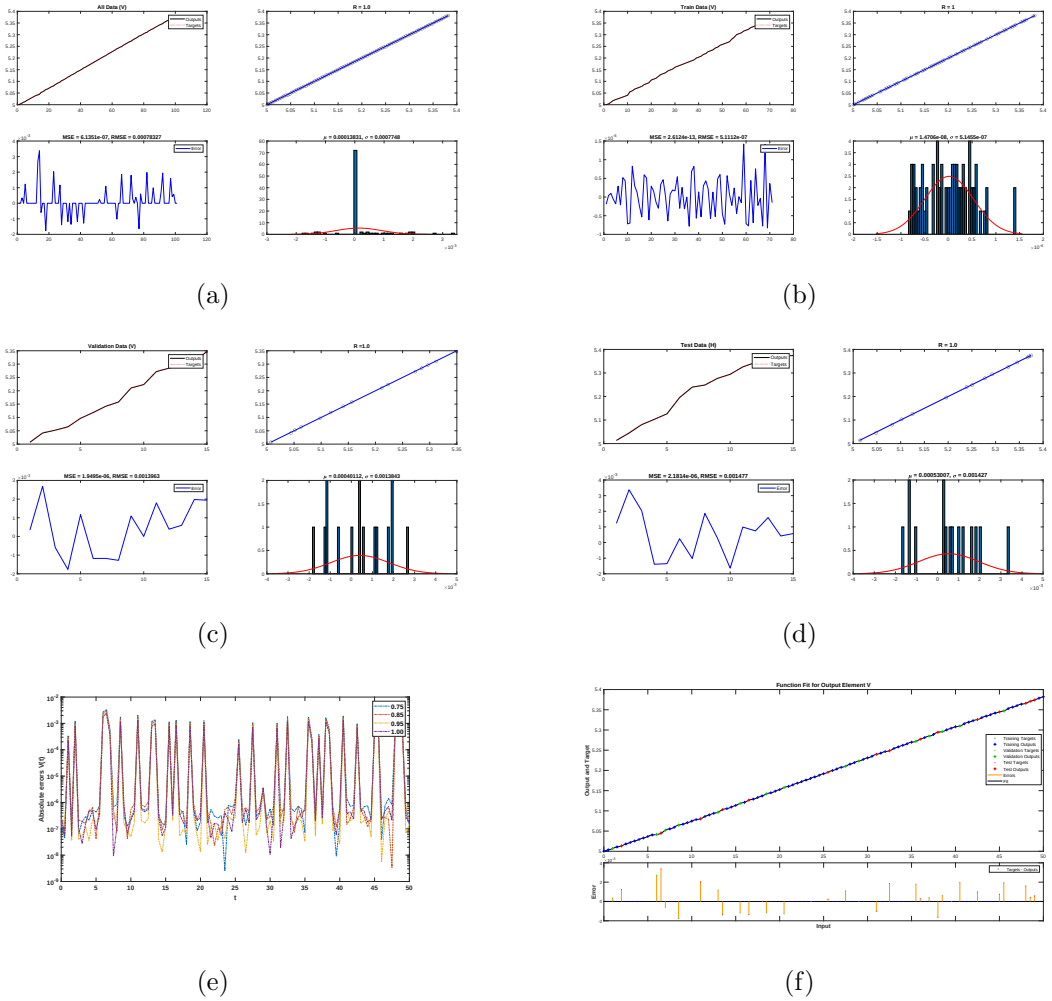

(a) (b)

(c) (d)

(e) (f)

Figure 8: Graphical presentation of various data results for class V using NNs (a) all data, (b) train data, (c) test data (d) validation (e) absolute error using NNs and (f) function fit performance.

The NNs used contain two hidden layers with 20 neurons, while other units are presented in table 2.

Unite	Initial value	stopped value	target value
Epoch	0	68	1000
Elapsed time	-	00:00:00	-
Performance	28.9	$5.26e-12$	0
Gradient	46.9	$1.4e-06$	$1e-07$
standard deviation	0.001	$1e-011$	$1e+10$
Validation checks	0	0	6

Table 3: Training progress presentation for class V.

7. Conclusion

A discrete version of hepatitis B and C mathematical model was investigated by using CFDO. Sufficient conditions were developed for the existence theory and stability analysis. Moreover, numerical illustrations for various densities including healthy cells, infected and virus free cells were presented against two different sets of fractional orders. Also some stability results for the corresponding equilibrium points were given. In addition, NNs scheme was established and different data dependence results by using the generated data from the numerical scheme given in Eq. (20) using the provided initial values. Various results related to MSE, RMSE, regression coefficient, and absolute errors for all three classes were investigated. From the obtained analysis, it has been found that NNs can be used as alternative powerful tools to investigate different epidemic diseases models. In the future, we will extend our results to more complex dynamical systems of hepatitis B and C mathematical models.

Conflict of interest

We have no conflict of interest.

Acknowledgements

The authors would like to acknowledge Prince Sultan University for paying the APC and valuable support.

References

[1] Ching Shan Chou and Avner Friedman. *Introduction to mathematical biology: modeling, analysis, and simulations*. Springer, 2016.

[2] MG Roberts and JAP Heesterbeek. *Mathematical models in epidemiology*, volume 215. EOLSS Abu Dhabi, United Arab Emirates, 2003.

[3] Shaher Momani, Ranbir Kumar, HM Srivastava, Sunil Kumar, and Samir Hadid. A chaos study of fractional sir epidemic model of childhood diseases. *Results in Physics*, 27:104422, 2021.

[4] A Isaacs and CH Andrewes. Spread of influenza. *British medical journal*, 2(4737):921, 1951.

[5] Ingrid A Binswanger, Komal J Narwaney, Jennifer C Barrow, Kathleen B Albers, Laura Bechtel, Claudia A Steiner, Jo Ann Shoup, and Jason M Glanz. Association between severe acute respiratory syndrome coronavirus 2 antibody status and reinfection: A case-control study nested in a colorado-based prospective cohort study. *Preventive Medicine Reports*, 37:102530, 2024.

[6] A Melo-Florián. Spanish flu: learnings for xxith century. *Medicine*, pages 1–8, 2025.

[7] Helen S Te and Donald M Jensen. Epidemiology of hepatitis b and c viruses: a global overview. *Clinics in liver disease*, 14(1):1–21, 2010.

[8] Don Ganem and Alfred M Prince. Hepatitis b virus infection -natural history and clinical consequences. *New England journal of medicine*, 350(11):1118–1129, 2004.

[9] Syed Asad Ali, Rafe MJ Donahue, Huma Qureshi, and Sten H Vermund. Hepatitis b and hepatitis c in pakistan: prevalence and risk factors. *International journal of infectious diseases*, 13(1):9–19, 2009.

[10] Maud Lemoine and Mark Thursz. Hepatitis c, a global issue: access to care and new therapeutic and preventive approaches in resource-constrained areas. In *Seminars in liver disease*, volume 34, pages 089–097. Thieme Medical Publishers, 2014.

[11] Ngan Hoe Lee and Kit Ee Dawn Ng. *Mathematical modelling: From theory to practice*, volume 8. World Scientific, 2015.

[12] Amit Huppert and Guy Katriel. Mathematical modelling and prediction in infectious disease epidemiology. *Clinical microbiology and infection*, 19(11):999–1005, 2013.

[13] Rafael Pantoja Rangel, MDLG Magaña, Ricardo Ulloa Azpeitia, and Elena Nesterova. Mathematical modeling in problem situations of daily life. *Journal of Education and Human Development*, 5(1):62–76, 2016.

[14] Piotr Ostalczyk. *Discrete fractional calculus: applications in control and image processing*, volume 4. World scientific, 2015.

[15] Abdulrahman Al-Khedhairi, Abdelalim A Elsadany, and Amr Elsonbaty. On the dynamics of a discrete fractional-order cournot–bertrand competition duopoly game. *Mathematical Problems in Engineering*, 2022(1):8249215, 2022.

[16] Amr Elsonbaty and AA Elsadany. On discrete fractional-order lotka-volterra model based on the caputo difference discrete operator. *Mathematical Sciences*, 17(1):67–79, 2023.

[17] Lan-Lan Huang, Ju H Park, Guo-Cheng Wu, and Zhi-Wen Mo. Variable-order fractional discrete-time recurrent neural networks. *Journal of Computational and Applied Mathematics*, 370:112633, 2020.

[18] Zai-Yin He, Abderrahmane Abbes, Hadi Jahanshahi, Naif D Alotaibi, and Ye Wang. Fractional-order discrete-time sir epidemic model with vaccination: Chaos and complexity. *Mathematics*, 10(2):165, 2022.

[19] Vasily E Tarasov and Valentina V Tarasova. Long and short memory in economics: fractional-order difference and differentiation. *arXiv preprint arXiv:1612.07903*, 2016.

[20] Yuexi Peng, Shaobo He, and Kehui Sun. Chaos in the discrete memristor-based system with fractional-order difference. *Results in Physics*, 24:104106, 2021.

[21] Fulai Chen and Yong Zhou. Existence and ulam stability of solutions for discrete fractional boundary value problem. *Discrete Dynamics in Nature and Society*, 2013(1):459161, 2013.

[22] Pauline Van den Driessche. Reproduction numbers of infectious disease models. *Infectious disease modelling*, 2(3):288–303, 2017.

[23] Zahura Khatun, Md Shahidul Islam, and Uttam Ghosh. Mathematical modeling of hepatitis b virus infection incorporating immune responses. *Sensors International*, 1:100017, 2020.

[24] Olga Igorevna Krivorotko, N Yu Zyatkov, and Sergey Igorevich Kabanikhin. Modeling epidemics: Neural network based on data and sir-model. *Computational Mathematics and Mathematical Physics*, 63(10):1929–1941, 2023.

[25] Behnam Nikparvar, Md Mokhlesur Rahman, Faizeh Hatami, and Jean-Claude Thill. Spatio-temporal prediction of the covid-19 pandemic in us counties: modeling with a deep lstm neural network. *Scientific reports*, 11(1):21715, 2021.

[26] Xiao Ning, Linlin Jia, Yongyue Wei, Xi-An Li, and Feng Chen. Epi-dnns: Epidemiological priors informed deep neural networks for modeling covid-19 dynamics. *Computers in biology and medicine*, 158:106693, 2023.

[27] Muhammad Sher, Kamal Shah, Zeeshan Ali, Thabet Abdeljawad, and Manar Alqudah. Using deep neural network in computational analysis of coupled systems of fractional integro-differential equations. *Journal of Computational and Applied Mathematics*, page 116912, 2025.

[28] Kamal Shah, Thabet Abdeljawad, Bahaaeldin Abdalla, and Zeeshan Ali. Analyzing a coupled dynamical system of materials recycling in chemostat systems with artificial deep neural network. *Modeling Earth Systems and Environment*, 11(5):1–14, 2025.

[29] Hasib Khan, Jehad Alzabut, and DK Almutairi. Applications of artificial intelligence for clusters analysis of uranium decay via a fractional order discrete model. *Partial Differential Equations in Applied Mathematics*, 13:101056, 2025.

[30] Hasib Khan, Jehad Alzabut, DK Almutairi, and Wafa Khalaf Alqurashi. The use of artificial intelligence in data analysis with error recognitions in liver transplantation in hiv-aids patients using modified abc fractional order operators. *Fractal & Fractional*, 9(1), 2025.